

Core-excited autoionizing states in the alkali metals*

D. J. Pegg, H. H. Haselton, R. S. Thoe, P. M. Griffin, M. D. Brown, and I. A. Sellin

University of Tennessee, Knoxville, Tennessee 37916

and Oak Ridge National Laboratory, Oak Ridge, Tennessee 37830

(Received 26 September 1974; revised manuscript received 2 June 1975)

An extension of projectile-electron spectroscopy to keV-energy alkali-metal beams has permitted the first observations of the energies of a number of optically forbidden core-excited autoionizing states of the alkali metals. For example, we have located the $(1s2s^2)^2S$ and the $(1s2p^2)^2D$ states of Li which lie at 56.31 ± 0.03 eV and 61.04 ± 0.03 eV, respectively, above the ground state. Energies for theoretically less-well-established doublet and quartet states in Na, Mg^+ , and K are also presented.

I. INTRODUCTION

Atoms and ions may frequently be excited to states which in turn spontaneously decay by electron rather than photon emission. Such a radiationless transition is called autoionization. For this process to be energetically possible, the excited state must be degenerate in energy with a state in some ionization continuum, i.e., the excitation energy of the state must be greater than the energy required to liberate a single outer-shell electron. The simultaneous excitation of two loosely bound outer-shell electrons or the excitation of a more tightly bound inner-shell electron to a higher orbital will satisfy this energy requirement. It is the latter process, which is known as core excitation, that has been studied in the present experiment. In general, there exist two types of autoionizing states: those which decay rapidly via the interelectronic electrostatic (Coulomb) interaction and those which are metastable against this allowed process but which autoionize at a slower rate via the weaker magnetic interactions. In all cases, the autoionization rate is determined by the magnitude of the matrix element connecting the core-excited state to the adjacent continuum. The discrete energy electron emitted in the process has a kinetic energy equal to the difference in binding energies of the initial core-excited state and that of the final state of the residual ion of the next higher charge state.

The literature concerning photoelectron, electron-impact, and ion-impact spectroscopy of autoionizing states of the permanent gases is extensive.¹ Similar results on the equally fundamental alkali metals are comparatively rare and usually of lesser accuracy, especially in the case of optically forbidden states. Presumably, one reason for this circumstance arises from the destructive attack of hot alkali-metal vapors on

critical spectrometer components, especially narrow, precisely machined spectrometer defining slits. We report here the first data on a number of optically forbidden core-excited states of Li, Na, Mg^+ , and K, and we present pertinent details of a method (projectile electron spectroscopy) which allows ready access to large numbers of such levels in many alkali and alkalilike systems and which in addition solves the hot-vapor-target problem. Preliminary results for Li and Na have been published.²

Earlier studies of core excitation in the alkali metals were made by Beutler and co-workers³ in the 1930's. Anomalous photoabsorption lines were observed in the ultraviolet continuum of several heavier alkali metals. The broadened lines suggested that the upper levels of the transitions involved, which lie far above the ionization limits of these atoms, autoionized rapidly. Recently, similar photoabsorption methods involving more sophisticated background sources have been used to obtain accurate binding energies of optically allowed core-excited states of most of the alkalis. Photoexcitation from the ground state of the alkali metals (involving a single photon) is, however, restricted to the excitation of optically allowed states, i.e., states optically connected by the $E1$ selection rules to the $^2S_{1/2}$ alkali ground states. Collisional excitation processes, such as those used in the present work, can serve to complement the photoabsorption studies, since they are not subjected to the same restrictions. Many optically forbidden states have been excited in the present work, along with optically allowed states; the precise energies of the latter, as measured by photoabsorption techniques, serve to establish an accurate absolute energy scale in the present experiments. Studies of metastable autoionizing states in the alkali metals were first reported by Feldman and Novick.⁴ Later, work at the Moscow State University⁵ and the Oak Ridge

National Laboratory⁶ extended the investigations to the more highly stripped members of the alkali isoelectronic sequences.

The binding energies of a number of core-excited states of several alkali systems have been the subject of calculations by Weiss,⁷ Holøien and Geltman,⁸ Garcia and Mack,⁹ Martin *et al.*,¹⁰ Junker,¹¹ Junker and Bardsley,¹² Nicolaides,¹³ and Gabriel.¹⁴ Most of these calculations, particularly those involving the heavier alkali metals, have uncertainties on the order of ± 0.1 eV, which are comparable to or exceed the presented estimated experimental uncertainties. Hence our data should be interpretable at theoretically useful levels of accuracy. Theoretical difficulties arise from the strong state mixing due to the spin-orbit interaction associated with the p vacancy in the noble-gas cores of the heavier alkali metals.

The role of direct inner-shell ionization and the excitation of inner-shell electrons (to autoionizing states) in the over-all ionization of sodiumlike ions by electron impact has been recently considered by both Bely¹⁵ and Moores and Nussbaumer.¹⁶ These calculations show that both of the aforementioned processes should produce significant contributions to the over-all ionization cross section vs electron impact energy, although there appears to be a disagreement as to the amount. It is evident that a better knowledge of the excitation thresholds of the autoionizing states would aid in such estimations. The present results for the energies of core-excited autoionizing states associated with the $2p^5 3s 3p$ configuration of Mg^+ are somewhat lower than the theoretical estimates of these quantities by Moores and Nussbaumer,¹⁶ for example. Goldberg *et al.*¹⁷ have pointed out that the autoionization process should be taken into account in the calculation of ionization rates involved in the physics of stellar atmospheres.

Another area of research in which a knowledge of the excitation energies of core-excited states is useful is in the study of the so-called satellite lines that are produced in laboratory and astrophysical plasmas. Such lines, when associated with lithiumlike ions, for example, lie on the long-wavelength side of the resonance lines of heliumlike ions, and are the result of radiative transitions from core-excited states to the ground state or to the normal excited states of the lithiumlike system which involve the excitation of the valence electron. This decay channel becomes relatively more probable for highly stripped members of the lithium sequence since the rate for such a process scales $\sim (Z - \sigma)^4$, whereas the rate for the allowed autoionization process is relatively independent of Z . Gabriel¹⁴ has pointed out that

in plasmas the contribution to the production of core-excited states through the process of dielectronic recombination can be important. Since this recombination process is sensitively dependent upon electron temperatures and densities, the study of satellite-line intensities is often useful as an effective probe of plasma temperature and density conditions.

Recently, Nikolaev *et al.*¹⁸ have shown that the autoionization process is responsible for a large apparent decrease in the measured capture cross sections for beams of heliumlike ions passing through thin gas targets when the incident beams have enriched metastable heliumlike-ion populations. The mechanism that the authors propose is that electrons are often captured into the states with $n \geq 2$ of the resultant lithiumlike ions, many of which have vacancies in the K shell. These core-excited states in turn rapidly autoionize, leaving a residual heliumlike ion in the ground state before a charge-state measurement can be made.

II. METHOD

The method of projectile electron spectroscopy has been used in the present work. In this technique spectroscopic measurements are made on the electrons emitted during the autoionizing decay in flight of collisionally excited atoms or ions which form a fast unidirectional beam. A schematic of the essential apparatus is shown in Fig. 1. Well-collimated and intense ($\sim 10 \mu A$) singly charged alkali-ion beams were obtained from the UNISOR facility (Universities Isotope Separator at Oak Ridge). This accelerator has a variable terminal voltage up to a maximum of 80 kV. The beams were passed at ~ 70 keV through a differentially pumped gaseous target cell, which served to both neutralize (if necessary) and collisionally excite the beam. Several different target gases and pressures were tried in the experiment, but it was found that He targets produced the best signal-to-background ratio in the electron spectra from the projectiles. Electrons emitted at a mean polar angle of 42.3° from a small section (length 0.15 mm, diameter 1.5 mm) of the excited beam were collected and energy analyzed by means of a cylindrical-mirror electrostatic analyzer. The dimensions of the inner and outer cylinders of this analyzer are 5.7 and 12.2 cm, respectively, and the dispersion of the instrument is ~ 32 cm. The analyzer has been described in greater detail in a recent article by Sellin.¹⁹ The spread in the polar angle of acceptance of the analyzer due to the finite size and spacing of the entrance slits was restricted in this instrument to 1.2 mrad in order to reduce spectral peak-

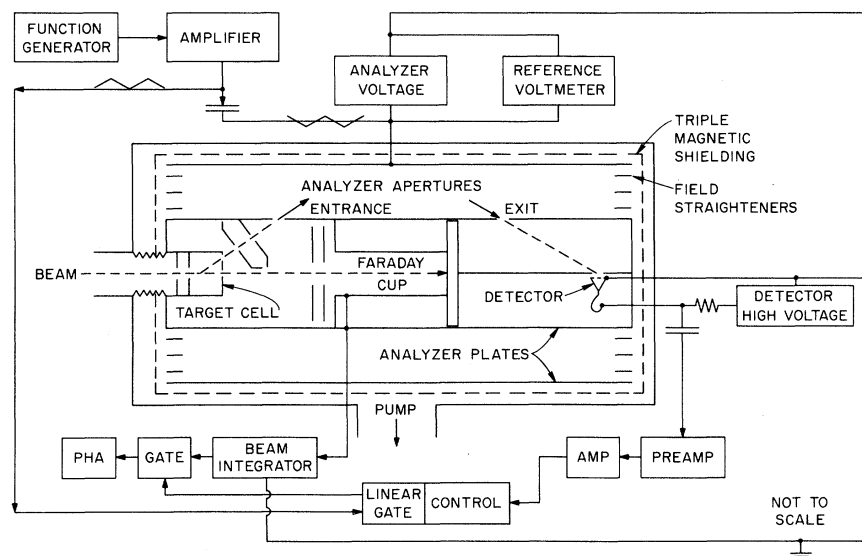


FIG. 1. Schematic diagram of the apparatus showing the cylindrical-mirror analyzer in a plane containing the beam axis. Radii of the inner and outer electrodes of the analyzer are 5.7 and 12.2 cm, respectively. Collisional excitation of the projectiles takes place in the differentially pumped gaseous target cell situated in the viewing region of the entrance-slit system.

broadening resolution loss due to kinematic effects, the most important source of resolution degradation. The severe collimation in the polar angle spread is partially compensated for having an azimuthal angle of acceptance of 120° . The spectra were scanned by applying a linear voltage ramp signal simultaneously to the outer electrode of the analyzer and to a divider chain linked to the linear input of a multichannel analyzer through a linear gate. The gate is opened by the signal pulses from an electron-multiplier detector located behind the spectrometer exit slit. More recently, we have found it preferable to replace the linear ramp generator with a 12-bit digital-to-analog converter system which simultaneously addresses the multiscaling input of a multichannel

analyzer and the input of a high-loop-gain well-regulated operational power supply which provides the analyzer voltage. Channel advance is controlled by a pulse from a beam-current digitizer. Fringe-field correction rings are spaced at logarithmic radial intervals between the inner and outer cylinders of the analyzer. A triple layer of annealed conetic magnetic shielding (thickness 1.27 mm) reduces the ambient magnetic field inside the spectrometer to a peak value of less than 10 mG and an average value under 3 mG. The entire spectrometer is housed in a vacuum chamber maintained at a residual pressure of $\sim 10^{-8}$ mTorr.

The analyzer constant and the instrumental resolution were obtained by using the well-established

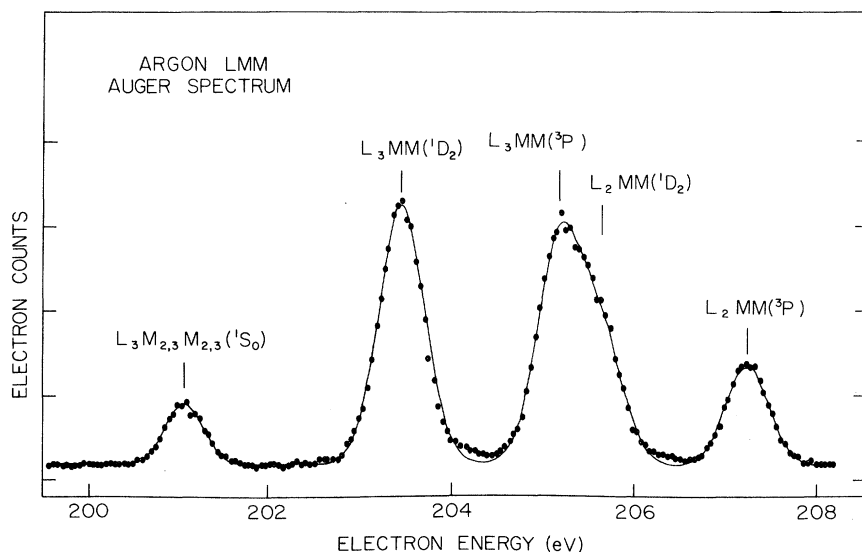


FIG. 2. Calibration spectrum of electron-impact excited *LMM* Auger transitions in argon with the cylindrical-mirror electrostatic analyzer used in the present experiments.

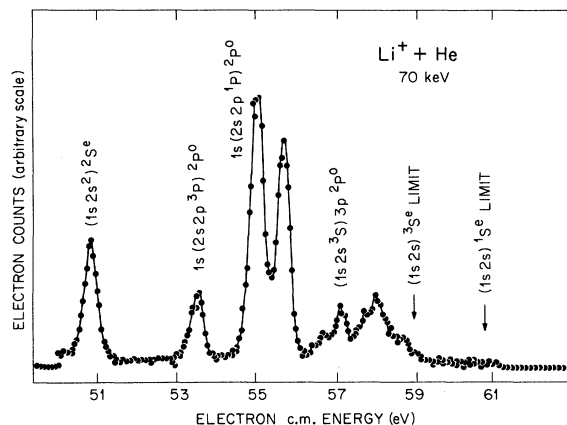


FIG. 3. Spectrum of electrons emitted by a beam of 70-keV lithium atoms undergoing autoionizing decay in flight following collisional excitation in a He-gas target. Electron energies are expressed with respect to the rest frame of the emitting atom. Corresponding excitation energies of the autoionizing states are obtained by adding the ionization potential of lithium (5.392 eV) to the electron peak energies.

TABLE I. Autoionizing states in lithium.

Excitation energy (eV)		Theory	Assignment
Present expt.	Other expt.		
56.31	...	56.43 ^a	(1s2s ²)2S
58.91	58.910 ^b	58.96 ^c	1s(2s2p ³ p)2P ⁰
60.40	60.396 ^b	60.60 ^c	1s(2s2p ¹ p)2P ⁰
61.04	...	62.0 ^d	(1s2p ²)2D
61.8
62.0
62.42	62.419 ^b	62.46 ^c	(1s2s ³ s)3p ² P ⁰
62.5
62.9
63.0
63.2
63.3	63.356 ^b	63.36 ^c	(1s2s ³ s)4p ² P ⁰
63.4
63.6
63.7
63.8	63.753 ^b	...	(1s2s ³ s)5p ² P ⁰
64.0
64.1
64.3

^a Reference 11.

^c Reference 7.

^b Reference 20.

^d Reference 13.

lished energies of electron-impact-excited Auger lines from the inert gases. Figure 2 shows a typical spectrum of *LMM* transitions in argon. Such target lines are, of course, far less broadened by kinematic effects than projectile lines, and in the case of the present data the analyzer was operated at a resolution of $\sim 0.2\%$.

One consequence of the small source volume determined by the stringent collimation conditions in the polar-angle spread is that the instrument is more sensitive to the observation of fast decaying states than states with lifetimes corresponding to decay lengths much larger than the entrance-slit window. The window attenuation factor $\Delta x/v\tau$, where Δx is the length of excited beam that is observed, v is the beam velocity, and τ is the lifetime of the state, is a measure of the probability of decay within the viewing region defined by

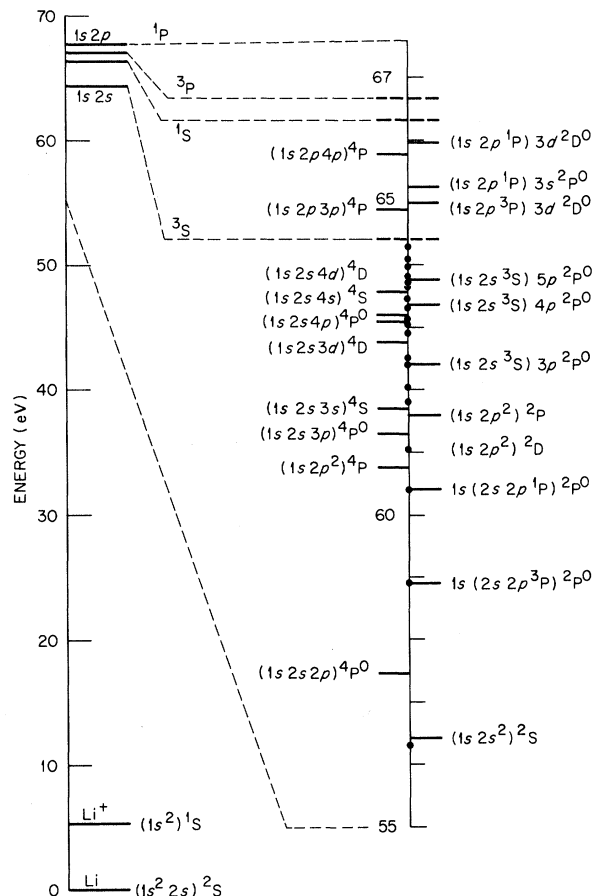


FIG. 4. Partial energy-level diagram of lithium indicating some core-excited states. Black dots shown on the expanded scale at the right indicate the present experimental measurements. Horizontal lines to the right and left of this expanded scale show the results of either calculations or photoabsorption experiments. All results are tabulated in Table I.

the entrance-slit system of the analyzer. This attenuation is apparent in the absence of the longer-lived metastable quartet states in our spectra of lithium, in contrast to our earlier observations⁶ of many lithiumlike quartet states in faster-decaying more highly stripped ions. The sensitivity of the apparatus to longer-lived states can of course be increased by increasing the length of beam observed, but only at the expense of loss of resolution. The beam velocity for a given experiment is chosen to produce a substantial component of the charge state of interest in the collision cell. In the present experiment, the states studied have lifetimes in the range 10^{-13} – 10^{-15} sec and consequently are formed and decay within the viewing region.

III. RESULTS

A. Lithium

Figure 3 shows a typical spectrum of electrons emitted by a 70-keV lithium beam undergoing

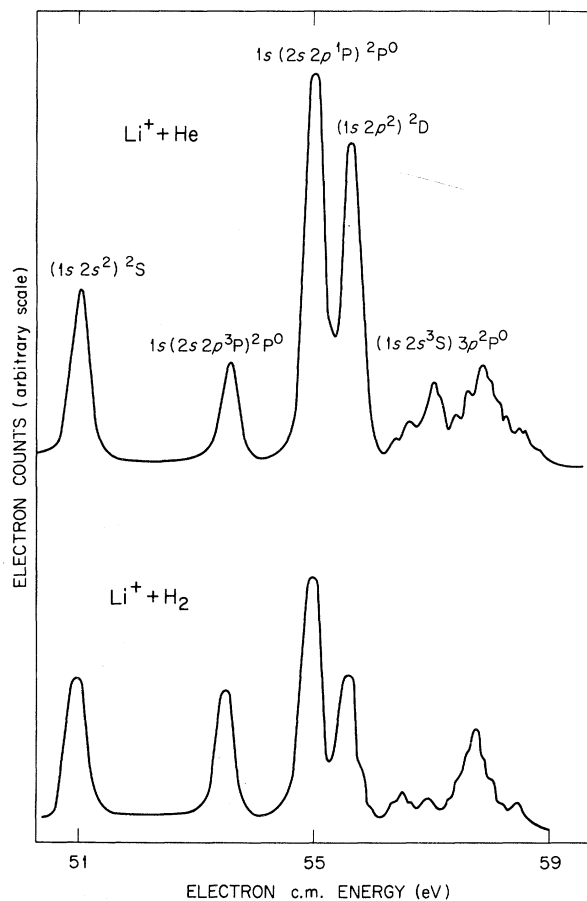


FIG. 5. Comparison of electron spectra obtained for 70-keV lithium ions incident upon equivalent (20 mTorr) He (top) and H_2 (bottom) gaseous targets. Changes in the relative intensities of some of the features are shown.

autoionizing decay in flight following collisional excitation in a He-gas target cell maintained at a pressure ~ 20 mTorr. The spectral features are associated with the allowed autoionizing decay of doublet states involving core-excited configurations of the type $1s2snl$ ($n \geq 2$) and $1s2pnl$ ($n \geq 2$) in which a hole exists in the K shell.

The lowest energy feature of the lithium spectrum arises from the autoionizing decay of the optically forbidden doublet $(1s2s^2)^2S$. The excitation energy of this state is measured to be 56.31 ± 0.03 eV, in agreement with a subsequent calculation of Junker¹¹ of 56.43 eV. The observed energies of the optically allowed $1s(2s2p^3P)^2P^0$, $1s(2s2p^1P)^2P^0$, and $(1s2s^3S)^3p^2P^0$ are in good agreement with the accurate photoabsorption results of Ederer *et al.*,²⁰ and such states have been used to establish an accurate absolute energy scale in the present work. The rather intense line in the spectrum corresponding to an excitation energy of 61.04 ± 0.03 eV appears to be associated with the decay of the optically forbidden $(1s2p^2)^2D$ state. Since this line was not reported by Ederer *et al.*,²⁰ it is expected to be the result of an optically forbidden transition (i.e., an upper

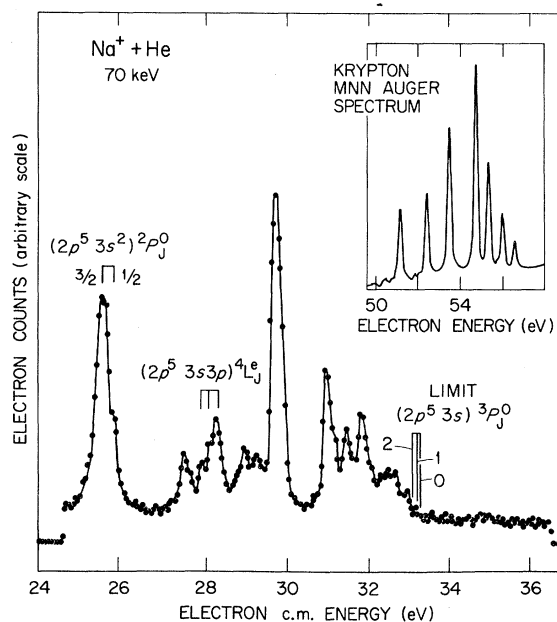


FIG. 6. Spectrum of electron emitted by a 70-keV sodium beam undergoing autoionizing decay in flight following collisional excitation in a He-gas target. Electron energies are expressed in the rest frame of the emitting atom. Corresponding excitation energies of the autoionizing states are obtained by adding the ionization potential of sodium (5.139 eV) to the electron peak energies. The inset shows a calibration spectrum of krypton Auger lines excited by electron impact.

TABLE II. Autoionizing states in sodium.

Excitation energy (eV)		Theory ^b	Assignment
Present expt.	Other expt. ^a		
30.77	30.768	30.88	$(2p^5 3s^2)^2 P_{3/2}^o$
31.0	30.934	31.35	$(2p^5 3s^2)^2 P_{1/2}^o$
32.67	...	32.72	$(2p^5 3s 3p)^4 S$
32.8	...		
33.08	...	33.09	$(2p^5 3s 3p)^4 D$
33.2	...		
33.38	...	33.32	$(2p^5 3s 3p)^4 P$
33.9	} $2p^5 (3s 3p^1 3P)^2 D, P, S$
34.1	
34.4	
34.79	
35.6	35.566	35.59	$(2p^5 3s^3 P) 4s^4 P$
35.8	35.768	35.79	$(2p^5 3s^3 P) 4s^2 P$
35.99	35.985	35.97	$(2p^5 3s^3 P) 3d^2 P$
36.1	36.129	36.17	$(2p^5 3s^1 P) 4s^2 P$ or $(2p^5 3s^3 P) 3d$
36.46	36.394	36.40	$(2p^5 3s^3 P) 4p$ or $(2p^5 3s^3 P) 3d$
36.82	$(2p^5 3s^3 P) 4p$ or $(2p^5 3s^3 P) 5s$
37.0	37.070	36.99	$(2p^5 3s^3 P) 4d$ or $(2p^5 3p^2)^4 P$
37.3	37.292	37.21	$(2p^5 3s^3 P) 5d$ or $(2p^5 3p^2)^4 D$
37.5	37.497	37.50	$(2p^5 3p^2)^4 S$
37.8	37.800	...	
38.1	

^a Reference 22.^b Reference 7.

state of even parity). The lowest-lying optically forbidden doublets above the $(1s2s^2)^2S$ state should be three doublets associated with the $1s2p^2$ configuration. The relative ordering of these states is 2D , 2P , 2S , a result which has been confirmed experimentally¹⁴ in studies of satellite spectra from more highly stripped members of the lithium sequence. The excitation energy of the $(1s2p^2)^2P$ state can be found from the beam-foil spectral data of Buchet *et al.*²¹ and is estimated to be 61.60 eV, implying that the state at 61.04 eV is probably the $(1s2p^2)^2D$ state. The $(1s2s3s)^4S$ state energy calculation of Holøien and Geltman,⁸ which provides a lower limit for the two doublet S states associated with this configuration, yields an excitation energy of 61.69 eV. Table I summarizes the results of the present measurements for lithium along with the photoabsorption data of Ederer *et al.*²⁰ and theoretical calculations of Weiss,⁷ Nicolaidis,¹³ and Junker.¹¹ The estimated accuracy of the present measurements are ± 0.03

eV for the intense and well-resolved lines, and ± 0.1 eV for the other features. There also appears to be a well-defined drop-off in intensity at an energy corresponding to the $(1s2s)^3S$ state of Li^+ , indicating that many of the states observed do converge to this limit. Many of the unidentified lines are probably associated with optically forbidden core-excited configurations of the type $(1s2s^3S)3s$, $(1s2s^1S)3s$, $(1s2s^3S)3d$, $(1s2s^1S)3d$, $(1s2p^2)^2S$, etc., whose energies have not as yet been calculated. Figure 4 shows a partial energy-level diagram of the lithium system in which the present measurements are indicated by the black dots on the expanded scale on the right side of the figure. Other experimental results and theoretical estimates are shown as horizontal lines to the right (doublets) and left (quartets) of the expanded scale, respectively.

Figure 5 demonstrates the change in the relative intensities of some of the spectral features resulting from a change in the nature but not of the

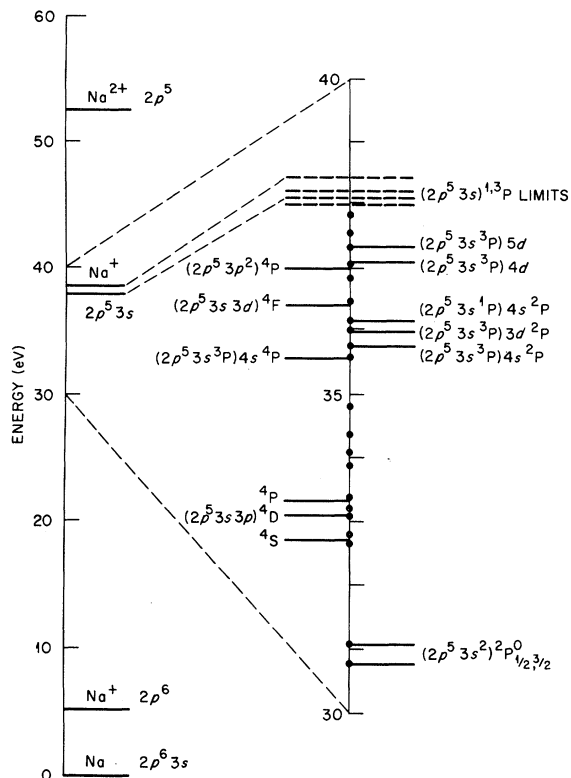


FIG. 7. Partial energy-level diagram of sodium showing some core-excited states. Black dots shown on the expanded energy scale at the right represent the present measurements. Results of calculations or photoabsorption studies are indicated by horizontal lines alongside the expanded energy scale. All results are tabulated in Table II.

pressures of the target gas. It is rather interesting to note the large relative change in the intensities of lines associated with the decay of the $(1s2p^2)^2D$ and $1s(2s2p^3P)^2P^o$ peaks, a phenomenon

currently lacking a plausible explanation. No quantitative study of how the relative intensities of the spectral lines depended upon the nature and pressure of the target gas was made at the present experiment, although future investigations of this intensity variation are planned.

B. Sodium

Figure 6 shows a spectrum of electrons emitted in the autoionizing decay in flight of a 70-keV sodium beam following collisional excitation in a differentially pumped He-gas target cell ($p \sim 20$ mTorr). The spectral features are associated with the decay of states formed from core-excited configurations of the type $2p^5 3snl$ ($n \geq 3$) or $2p^5 3pnl$ ($n \geq 3$), in which a vacancy exists in the L shell. Accurate photoabsorption results of Wolff *et al.*²² for the energies of optically allowed states such as $(2p^5 3s^2)^2P^o$ and $(2p^5 3s^3P)3d$ have been used to establish the energy scale for this spectrum. The major new feature in the sodium spectrum appears to be the presence of a group of optically forbidden states associated with the core-excited configuration $2p^5 3s3p$. The present measurements agree quite well with the superposition-of-configurations (SOC) calculation of Weiss⁷ for the energies of the 4S , 4D , and 4P states of the $2p^5 3s3p$ configuration. In addition to these assignments, it appears that we observe the decay of the six doublets arising from the $2p^5 3s3p$ configuration for which theoretical estimates are not presently available. The computational difficulties which arise in calculations of the energies of core-excited states in the alkali metals heavier than lithium stem from the rather strong spin-orbit interaction associated with the vacancy in the p subshell of these atoms, a situation which can imply considerable state mixing and an eventual breakdown of the LS coupling

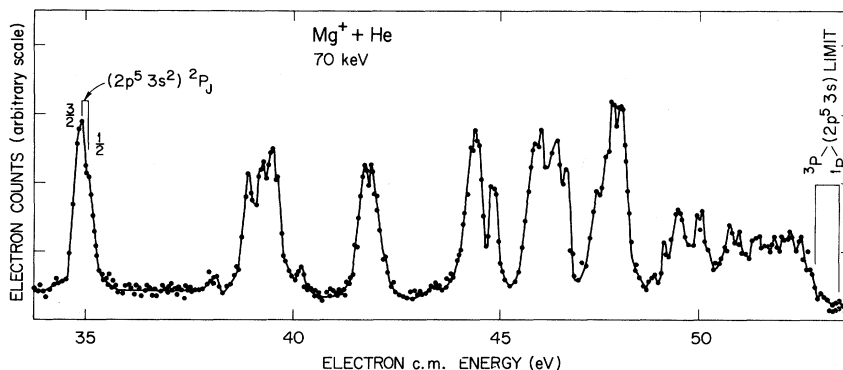


FIG. 8. Spectrum of electrons emitted by 70-keV magnesium atoms and ions undergoing autoionizing decay in flight following collisional excitation in a He-gas target. Electron energies are expressed in the rest frame of the emitting atoms or ions. Corresponding excitation energies of autoionizing states in singly ionized magnesium are obtained by adding the Mg^+ ionization potential (15.035 eV) to the energies of the electron peaks shown.

TABLE III. Autoionizing states of singly ionized magnesium.

Excitation energy (eV)		Theory ^b	Assignment
Present expt.	Other expt. ^a		
49.90	49.898	50.24	$(2p^5 3s^2)^2 P_{3/2}$
50.1	50.166	...	$(2p^5 3s^2)^2 P_{1/2}$
53.2	...	53.25	$(2p^5 3s 3p)^4 S$
53.9	...	53.95	$^4 D$
54.3	...	54.38	$^4 P$
54.5	...	54.55	$2p^5 (3s 3p^3 I)^2 D$
54.7	...	54.74	$^2 P$
55.2	...	55.34	$^2 S$
56.8	...	57.03	$2p^5 (3s 3p^1 P)^2 D$
57.1	...	57.19	$^2 P$
57.3	...	57.39	$^2 S$
57.8	
59.3	59.30	...	$(2p^5 3s^3 P) 4s^2 P$
59.5	$(2p^5 3s^3 P) 3d^2 P$
59.8	$(2p^5 3s^1 P) 4s$ or $(2p^5 3s^3 P) 3d$
60.9	60.92	...	$(2p^5 3s^3 P) 3d$
61.4	61.38	...	$(2p^5 3s^1 P) 3d$
61.5	$2p^5 3s 4p$ or $(2p^5 3s^3 P) 5s$

^a Reference 24.^b Reference 7.

scheme for some configurations. However, Connerade *et al.*²³ have pointed out that it appears for their photoabsorption data that the *LS* coupling scheme may still be substantially valid for many core-excited configurations of the sodium atom. The effect of this strong spin-orbit interaction can be seen in the spectra in the partially resolved structures caused by the comparatively large fine structure [~ 0.16 eV for the splitting of the levels arising from the $(2p^5 3s^2) p^o$ term] and in the presence of quite strong lines arising from the decay of states which are at least partially quartet in character. These "quartet" states are metastable against autoionization in the *LS* coupling approximation but become much shorter lived in these systems, because of mixing with fast decaying doublets of the same parity and total angular momentum as well as increases in the rates for forbidden autoionization processes brought about by the magnetic interactions. Table II summarizes the present results for sodium along with the photoabsorption measurements of Wolff *et al.*²² and the theoretical predictions of Weiss.⁷ The estimated accuracy of the present measurements is ± 0.1 eV for most of the lines. Again, there appears to be a rather well-defined

drop in activity at an energy corresponding to the expected series limit of $(2p^5 3s)^3 P$. The results are also shown in Fig. 7, which shows a partial energy diagram for sodium. The black dots on the expanded scale to the right indicate the present measurements, and the horizontal lines to the right and left of this scale are the results of either photoabsorption data or theoretical estimates.

C. Singly ionized magnesium

Figure 8 shows a typical spectrum of electrons emitted in the autoionizing decay in flight of core-excited states associated with atoms and ions in a 70-KeV collisionally excited magnesium beam. Most of the features are due to the decay of core-excited states associated with the sodiumlike fraction of the beam, i.e., singly ionized magnesium which forms a large component of the excited beam. A few features at higher electron energies can be associated with analogous states in neutral magnesium. Basically, the spectrum should be similar to that of sodium, with further increases in the size of the fine-structure splittings and state mixing effects. The photoabsorption measurements on optically allowed transitions by

Esteva and Mehlmann²⁴ determine the energy scale used in the present work. There is good agreement in most instances between the present results for the energies of the three quartets and six doublets associated with the optically forbidden $2p^5 3s 3p$ configuration and the SOC calculations of Weiss.⁷ The present results are tabulated in Table III along with Weiss's calculations and the photoabsorption data of Esteva and Mehlmann.²⁴ The estimated accuracy of the present results is ± 0.1 eV. Figure 9 shows a partial energy diagram for neutral and singly ionized magnesium. Again, the black dots indicate the present measurements, and the horizontal lines to the left (Mg) and right (Mg^+) of the expanded scale represent either photoabsorption or theoretical results. The spectrum in Fig. 8 is richer than that of neutral sodium owing to the presence of lines due to the autoionizing decay of core-excited

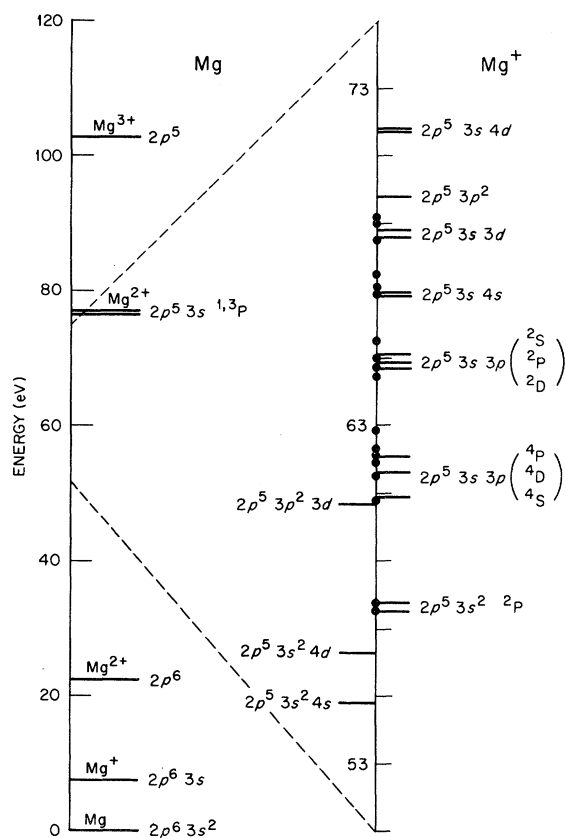


FIG. 9. Partial energy-level diagram of magnesium and singly ionized magnesium showing some core-excited states. Black dots on the expanded energy scale on the right represent the present measurements. Calculations and photoabsorption results for Mg and Mg^+ are shown as horizontal lines to the left and right of the expanded scale, respectively. All results are tabulated in Table III.

states of neutral magnesium of the type $2p^5 3s^2 nl$ ($n \geq 3$). Whereas the final state of the residual ion after decay in the case of singly ionized magnesium can only be the ground state of double ionized magnesium, i.e., $(2p^6)^1S$, there can be a number of final states of the residual Mg^+ ion following the autoionizing decay of a core-excited state in neutral magnesium.

D. Potassium

The spectrum of the autoionizing decay of core-excited states of potassium following the passage of a 70-keV K^+ beam through a He-gas target cell is shown in Fig. 10. It can be seen that the spectrum is exceedingly rich in lines, most of them incompletely resolved from one another. The lines present in the spectrum represent the autoionizing decay of states formed from core-excited configurations of the type $3p^5 4s nl$ ($n \geq 3$), $3p^5 3d nl$ ($n \geq 3$), $3p^5 4p nl$ ($n \geq 3$), etc. Since there has been little work, either experimentally or theoretically, on the core-excited states of potassium, it is difficult to assign an accurate energy scale. The energy scale shown in the figure is based upon the likely supposition that the two peaks indicated are associated with the $J = \frac{1}{2}$ and $\frac{3}{2}$ levels of the optically allowed term $(3p^5 4s^2)^2P^o$, which have been observed in earlier photoabsorption work by Beutler *et al.*³ and more recently by Hudson and Carter.²⁵ The fine-structure splitting between these two levels in our spectrum is in good agreement with the photoabsorption data. Martin *et al.*¹⁰ attempted to calculate the energies

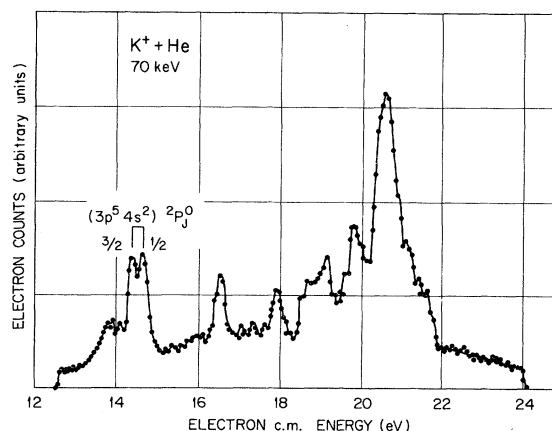


FIG. 10. Spectrum of electrons emitted by a 70-keV beam of potassium atoms undergoing autoionizing decay in flight following collisional excitation in a He-gas target. Electron energies are expressed in the rest frame of the emitting atom. Corresponding excitation energies of autoionizing states are obtained by adding the ionization potential of potassium (4.341 eV) to the peak energies.

of states associated with the $3p^5 4s 3d$ configuration. This work indicates the very strong departures from the LS coupling scheme involved in this type of configuration in potassium. The authors also predict that configurations such as $3p^5 4p^2$, $3p^5 3d^2$, $3p^5 4snl$ ($n \geq 4$), $3p^5 3dnl$ ($n \geq 4$), and $3p^5 4pnl$ ($n \geq 4$) either overlap or fall slightly above the higher levels of the $3p^5 4s 3d$ configuration, and, in addition, that configuration interaction would considerably enrich the spectrum. Of the core-excited systems whose energy levels have been discussed in this paper, the spectrum of potassium levels is by far the most in need of theoretical interpretation.

IV. SUMMARY

We have measured the energies of optically inaccessible and fundamentally important core-excited states in neutral and near-neutral alkali systems. Such work complements accurate photo-absorption studies on optically allowed states.

The method used in the experiments, projectile electron spectroscopy, avoids the problems associated with the use of a hot alkali-vapor target in the vicinity of the spectrometer. The present resolution level permits some state energy measurements that are better by a factor of 3 than corresponding energy calculations. A need for further calculations on Li and Na is evident, since the origin of a number of spectral features is still unknown. A similar but greater imbalance exists in the data on Mg^+ and K. In view of surprisingly large relative peak intensity variations, it is probable that interesting collision-mechanism information will emerge from more systematic variations of the nature and pressure of the target gas.

Note added in proof. Since submitting this manuscript, it has come to our attention that P. Ziem, U. Leithäuser, and N. Stolterfoht have performed overlapping experiments on Li core-excited states excited by H^+ and He^+ impact. An account of this work may be found in Ref. 26.

*Research supported in part by NSF, by ONR, by UNISOR (a consortium of fourteen institutions supported by them and by the ERDA), and by Union Carbide Corporation under contract with the U. S. ERDA.

¹For example, K. Siegbahn, C. Nordling, A. Fahlman, R. Nordberg, K. Hamrin, J. Hedman, G. Johansson, T. Bergmark, S. Karlsson, I. Lindgren, and B. Lindberg, *ESCA: Atomic, Molecular and Solid State Structure Studied by Means of Electron Spectroscopy* (Almqvist and Wiksells, Uppsala, Sweden, 1967); T. Carlsson, W. E. Moddeman, and M. O. Krause, *Phys. Rev. A* **5**, 1406 (1970); M. E. Rudd, *Phys. Rev. Lett.* **13**, 503 (1964).

²D. J. Pegg, H. H. Haselton, R. S. Thoe, P. M. Griffin, M. D. Brown, and I. A. Sellin, *Phys. Lett.* **50A**, 447 (1975).

³H. Beutler, *Z. Phys.* **91**, 131 (1934); H. Beutler and K. Guggenheimer, *Z. Phys.* **87**, 188 (1933).

⁴P. Feldman and R. Novick, *Phys. Rev. Lett.* **11**, 278 (1963); *Phys. Rev.* **160**, 143 (1967).

⁵I. S. Dmitriev, V. S. Nikolaev, and Ya. A. Teplova, *Phys. Lett.* **26A**, 122 (1968).

⁶B. Donnally, W. W. Smith, D. J. Pegg, M. D. Brown, and I. A. Sellin, *Phys. Rev. A* **4**, 122 (1971); I. A. Sellin, D. J. Pegg, M. D. Brown, W. W. Smith, and B. Donnally, *Phys. Rev. Lett.* **27**, 1108 (1971); D. J. Pegg, I. A. Sellin, P. M. Griffin, and W. W. Smith, *Phys. Rev. Lett.* **28**, 1615 (1972).

⁷A. W. Weiss (private communication).

⁸E. Holóien and S. Geltman, *Phys. Rev.* **153**, 81 (1967).

⁹J. D. Garcia and J. E. Mack, *Phys. Rev.* **138**, A987 (1965).

¹⁰W. C. Martin, J. L. Tech, and M. Wilson, *Phys. Rev.* **181**, 66 (1969).

¹¹B. R. Junker (private communication).

¹²B. R. Junker and J. N. Bardsley, *Phys. Rev. A* **8**, 1345 (1973).

¹³C. Nicolaidis, *Nucl. Instrum. Meth.* **110**, 231 (1973).

¹⁴A. H. Gabriel, *Mon. Not. R. Astr. Soc.* **160**, 99 (1972).

¹⁵O. Bely, *J. Phys. B* **1**, 23 (1968).

¹⁶D. L. Moores and H. Nussbaumer, *J. Phys. B* **3**, 161 (1970).

¹⁷L. Goldberg, A. K. Dupree, and J. W. Allen, *Ann. Astrophys.* **28**, 589 (1965).

¹⁸V. S. Nikolaev, I. S. Dmitriev, Yu. A. Tashaev, Ya. A. Teplova, and Yu. A. Fainberg, *J. Phys. B* **8**, L58 (1975).

¹⁹I. A. Sellin (unpublished).

²⁰D. L. Ederer, T. Lucatorto, and R. P. Madden, *Phys. Rev. Lett.* **25**, 1537 (1970).

²¹J. P. Buchet, M. C. Buchet-Poulizac, H. G. Berry, and G. W. F. Drake, *Phys. Rev. A* **7**, 922 (1973).

²²H. W. Wolff, K. Radler, B. Sonntag, and R. Haensel, *Z. Phys.* **257**, 353 (1972).

²³J. P. Connerade, W. R. Garton, and M. W. Mansfield, *Astron. J.* **165**, 203 (1971).

²⁴J. M. Esteve and G. Mehlmann, *Astron. J.* **193**, 747 (1974).

²⁵R. D. Hudson and V. L. Carter, *J. Opt. Soc. Am.* **57**, 1471 (1967).

²⁶See the *Abstracts of the Ninth International Conference on the Physics of Electrons and Atomic Collisions, Seattle, 1975*, edited by J. Risley and R. Geballe (Washington U.P., Seattle, Wash., 1975), Vol. 2, p. 865.